GLOBAL JOURNAL OF GEOLOGICAL SCIENCES VOL. 2, NO. 2, 2004: 207 - 220
COPYRIGHT(C) BACHUDO SCIENCE CO. LTD. PRINTED IN NIGERIA. ISSN 1596 - 6798

LABORATORY MODELLING OF GEOELECTRIC RESPONSE OF A LEAKING UNDERGROUND PETROLEUM STORAGE TANK IN SAND FORMATION.

O. AFOLABI and M. O. OLORUNFEMI

(Received 11 September, 2002; Revision Accepted 26 January, 2004)

ABSTRACT

Laboratory modelling of a simulated subsurface hydrocarbon impacted sand was carried out using a model tank. A crude oil filled metallic cylindrical tank (simulating a typical crude / refined hydrocarbon storage tank) was buried in the sand and pre-impact resistivity measurements with various electrode arrays (Wenner, dipole-dipole and gradient) were carried out along seven traverses, three of which traversed the buried cylindrical tank.

A subsurface impact via crude oil leakages from the sides of the cylinder was initiated and post-impact resistivity measurements were made with same electrode arrays and along the same traverses. The study was aimed at generating characteristic geoelectric signatures or patterns for the pre-impact and post-impact hydrocarbon-impacted sand.

Results from the resistivity profiles, maps and pseudosections as well as the inversion of the dipole-dipole data indicate diagnostic relatively high resistivity anomalies over the hydrocarbon-impacted zone.

Although the three electrode arrays resolved the lateral extent of the impacted zone, a combined horizontal/vertical profiling involving dipole-dipole array proved more useful in determining the lateral and vertical extent, i.e., the geometry of the contaminated zone. It also enabled an approximate estimation of the volume of leaked hydrocarbon. Apart from resolving the hydrocarbon-impacted zone, the method also identified the source of impact.

KEY WORDS: Subsurface, Leakage, Resistivity, Anomaly.

INTRODUCTION

Crude oil and its refined products have become invaluable in today's society. The environmental impact of oil spills has been a major problem in Nigeria, especially in the oil producing communities. The environmental impact of oil can be classified into two categories; burnt pollution and spillage pollution. The latter occurs at both the surface and subsurface. Surface oil pollution is mainly as a result of oil spills, which usually result from oil well blowout, pipeline rupture or tanker collision. Subsurface pollution on the other hand is due mainly to oil well blowout and underground leakages.

Spillage pollution, both surface and subsurface has far reaching effects on human, livestock, vegetation, forestry, wildlife, aquatic life, land use, soil and agriculture, climate and air quality. The effect of underground leakages have a more direct impact on man as it pollutes the underground water, which is an important source of potable water in most countries. According to Akinluyi (2000), hydrocarbons spread as a separate layer as well as in solution and in porous permeable formations. Pollution by a free product affects areas of the order of tens of metres in lateral extent, while the hydrocarbon in solution penetrates to distances of hundreds of metres or even kilometers. In fissured rocks, the spreading can be more complex. Hence the need for the early discovery and immediate remediation.

Nigeria in recent years has witnessed the rapid proliferation of petrol stations in many parts of the country (particularly cities like Lagos, Ibadan, Abuja, Port-Harcourt and many others). Preliminary study to determine the nature of the immediate environment in which storage tanks are buried i.e., acquisition of baseline data for future auditing of the subsurface in the vicinity of the tanks in accordance with the Federal Environmental Protection Agency (FEPA) is very rarely carried out. Failure of storage tanks at filling stations is known to have occurred in various parts of the country. This has led to heavy contamination of groundwater in the areas where such failures occur. Worst hit are some areas in Ajegunle and Ipaja, both in Lagos State (e.g., Olorunfemi, 2001). The immediate consequence of the impact is the pollution of the groundwater resource.

The investigation of hydrocarbon-impacted area may involve direct drilling or the use of non-invasive methods such as remote sensing, geobotany aerial photography and geophysics. The delineation of the extent of hydrocarbon contamination by drilling can be time consuming and difficult due to the often large extent of coverage, underground and aerial transmission lines and pipeline (Svoma, 1978). Nowadays geophysics has found excellent application in environmental investigations. The basic reasons for the use of geophysical methods to investigate environmental problems, particularly hydrocarbon spillage, are two fold. One is that geophysical methods can be used to evaluate the extent of existing problems. The other is that it can be used to predict where pollutants will go in the subsurface, and guide exploratory drilling programmes. It has been showed that carefully designed geophysical investigations can be employed to characterize hydrocarbon spill sites (Sauck et.al.,1998; Atekwana et.al., 2000; Olorunfemi et. al., 2001). In

O. AFOLABI, Department of Geology, Obafemi Awolowo University Ile - Ife, Nigeria
M. O. OLORUNFEMI, Department of Geology, Obafemi Awolowo University Ile - Ife, Nigeria

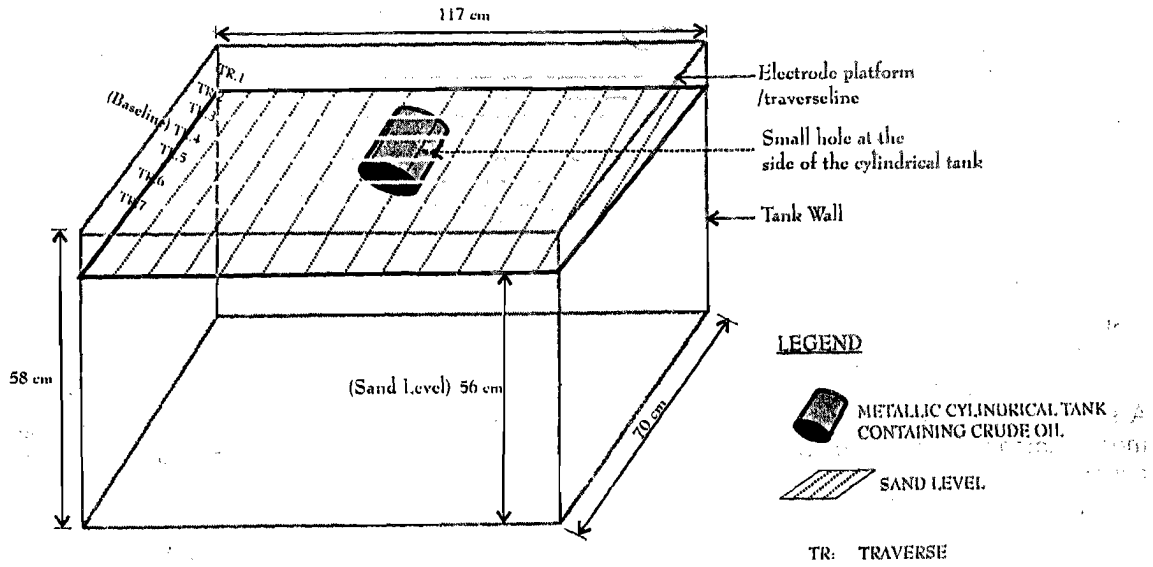

Fig. 1 : Schematic illustrationof the laboratory model tank showing measurement traverses.

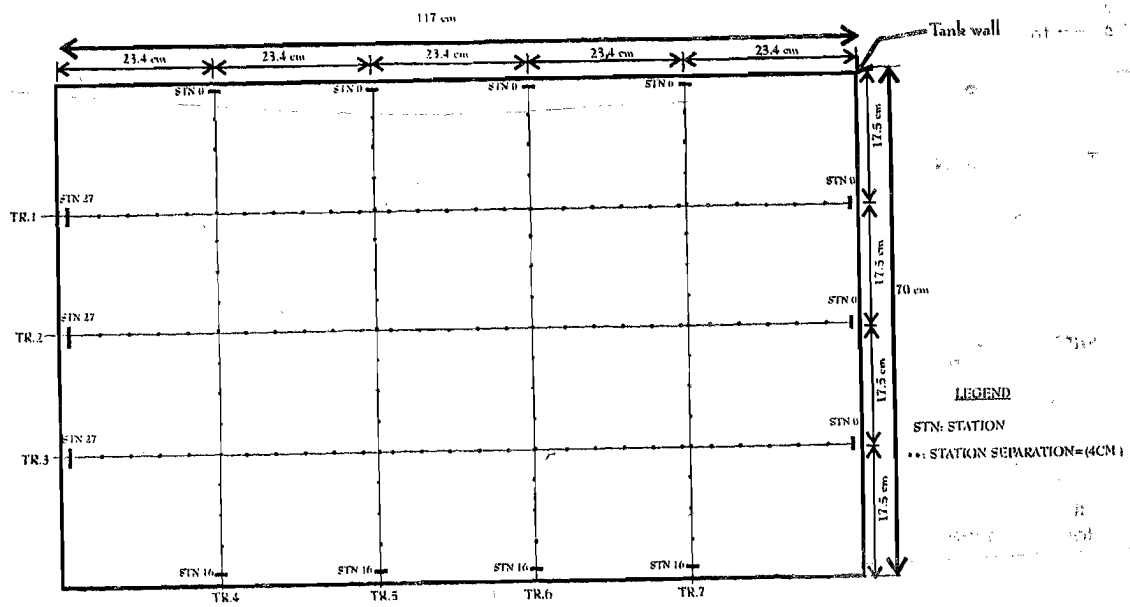

Fig. 2 : Traverse layout map for the wall effect measurement.

principle, all geophysical methods (i.e., Gravity, Magnetic, Seismic, Electrical, Electromagnetic, Ground Penetrating Radar (GPR), Radioactivity, Geothermal and Geophysical Borehole Logging) can be used for environmental studies (Mazac et al., 1987; Steeples, 1991; Gibson et al., 1996; Vickery and Hobb, 1998). However, the suitability of a particular geophysical method or a combination of methods for pollution studies depends very much on the physical property contrasts involved between the target structure and the surroundings, depth extent of the target, and the nature and thickness of the overburden. The most commonly used methods include: Magnetic, Seismic, Ground Penetration Radar (GPR) and Electrical / Electromagnetic methods.

The specific objectives of the present study are to. (i) generate characteristic geoelectric signatures or patterns for three commonly used electrode arrays over a buried petroleum storage tank prior to leakage and after leakage, (ii) evaluate the sensitivity of the electrode arrays to the hydrocarbon-impacted zone and (iii) determine which of the three electrode arrays resolve the hydrocarbon impacted zone better both spatially and vertically. An experimental approach was adopted in which a tank was constructed, filled with well-sieved sand, and a metallic cylindrical tank (filled with crude oil) to which two holes were drilled at opposite sides was buried in it. Apparent resistivity measurements were made with Wenner, dipole-dipole and gradient arrays. The sand body was then contaminated with crude oil after a leakage was initiated from the two holes at the sides of the buried tank and the apparent resistivity measurements repeated. A qualitative impression of the effect of the crude oil was obtained by comparing the

apparent resistivity profiles and maps of the pre-impacted and post-impacted sand. A quantitative model of the oil contamination was also developed by inverting the dipole-dipole apparent resistivity data.

METHOD OF STUDY

Laboratory scale modelling studies is often carried out, especially in new frontiers when the characteristic or signature produced by a particular effect is to be investigated. Applied geophysics takes the advantage that the response of natural field situations can be duplicated in the laboratory on a small convenient scale. Laboratory modelling is necessitated in areas of complex geology and limited number of geophysical and geological controls mainly to develop better understanding of geophysical responses of similar geologic setting, provide basis for an optimum

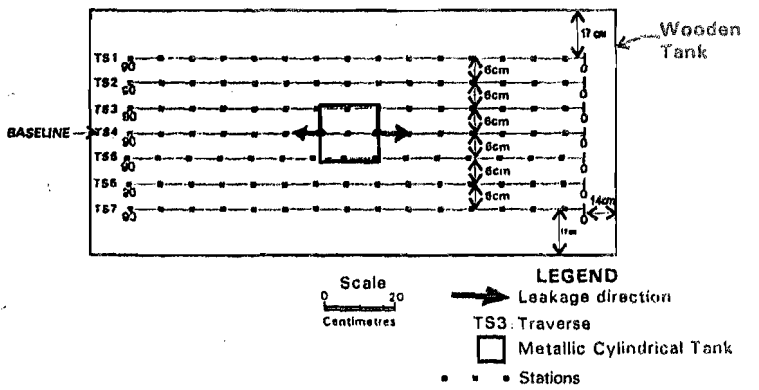

Fig. 3: Map of the tank showing the layout of the traverses

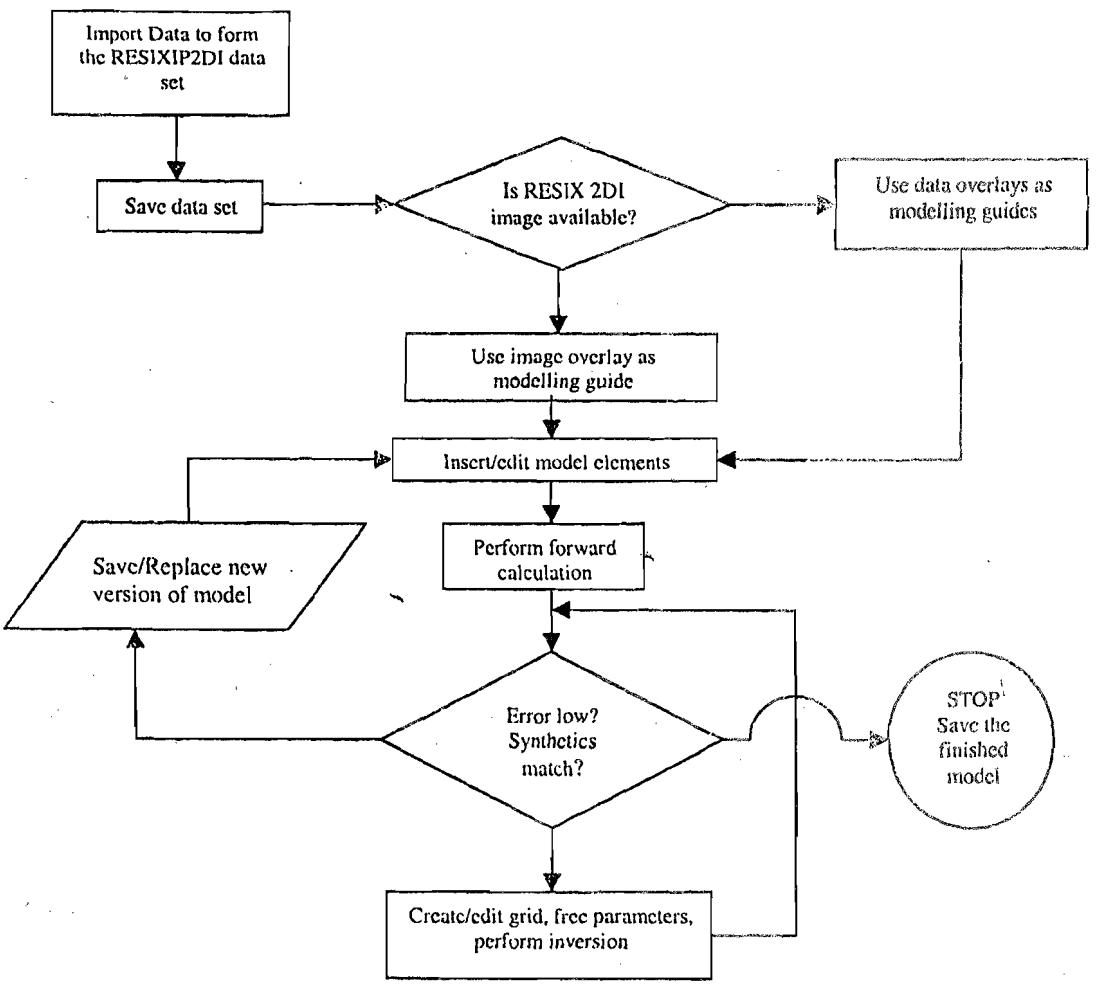

Figure 4: The flowchart showing the steps involved in producing a model using the RESIXIP2DI software.

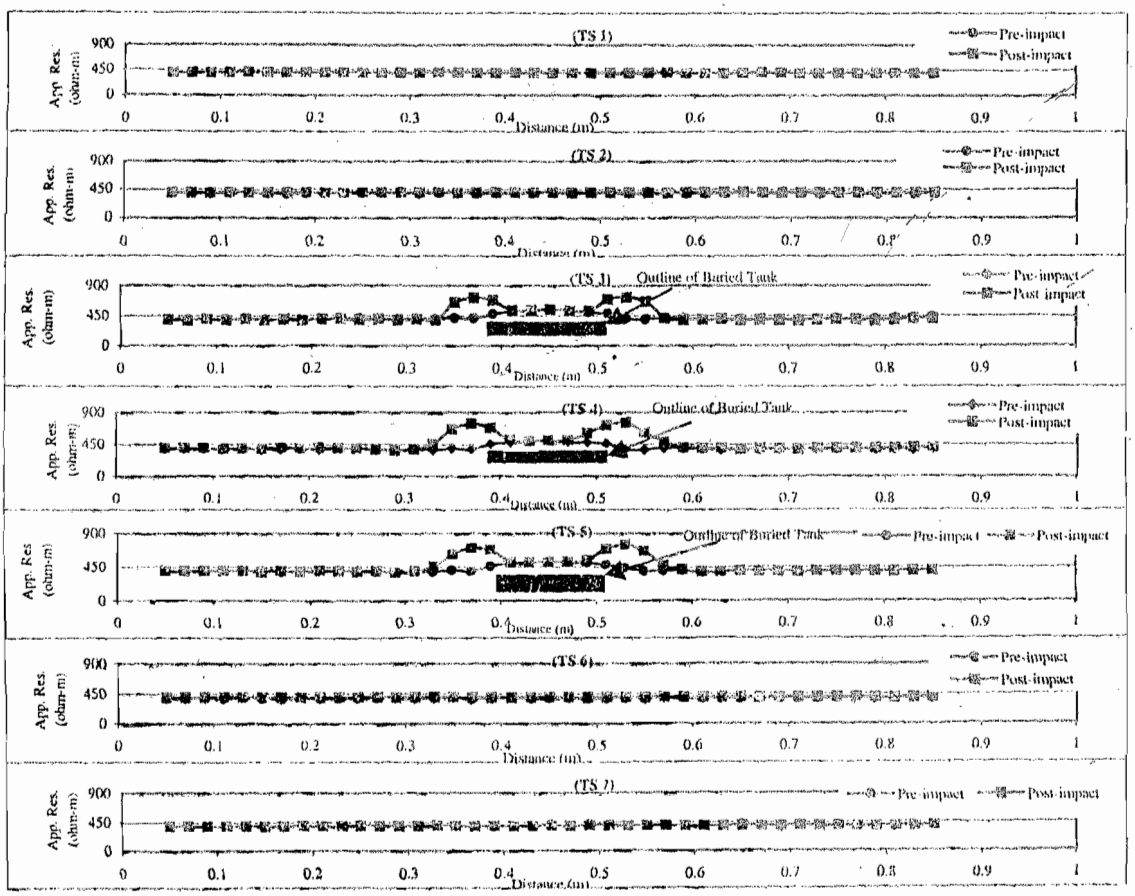

Fig. 5: Wenner resistivity (a=4 cm) profiles.

exploration strategy; and as an aid in interpretation (Olorunfemi et. al., 2001).

A simulated oil spill tank was carefully constructed in the Department of Geology Obafemi Awolowo University, Ile-Ife (Akinluyi, 2000). The model tank was made up of plank whose dimensions are 117 cm x 70 cm x 58 cm (Fig. 1) strong enough to withstand the pressure of the sand-fill. The interior wall was lined with polythene to prevent seepage of saturating fluid. And sieved river valley sand (less than 500 microns in diameter) was used to fill the model tank to a height of 56 cm. The tank was subsequently saturated with tap water.

A wooden board perforated at every 1 cm interval was used as electrode platforms for horizontal measurements. Two small holes of about 1 cm diameter were drilled on the opposite sides of a metallic cylindrical tank of length 17.3 cm and 13.2 cm diameter. Two rubber stoppers to which a strong string each had been attached was used to temporarily block the holes on the sides of the cylinder which was then filled with crude oil and buried lengthwise within the sand in the wooden tank such that the top surface of the cylindrical tank is at 2.5 cm depth. Some of the crude oil in tank was later allowed to leak into the sand by pulling out the stoppers blocking the holes on the sides of the cylindrical tank. Copper electrodes were used with digital ABEM SAS 300C Terrameter resistivity meter to determine the apparent resistivity at the various stations.

Three stages of measurements were carried out namely, wall effect test, pre-hydrocarbon impact measurement and post hydrocarbon impact measurement. The model tank being made of very resistive plank could be expected to influence the apparent resistivity response of its immediate surroundings. In other to determine the area within the tank whose apparent resistivity response would be least influenced by the resistive wall of the tank, a wall effect test was carried out. This involved running resistivity profiles, with the Wenner array, along three main traverses (TR1– TR3) and four orthogonal traverses (TR4 – TR5) as shown in Fig. 2. The inter-electrode spacing and station interval was 2 cm. As would be expected, local high apparent resistivities about double the average, within the tank, were observed in the vicinity of the walls of the tank. This relatively high apparent resistivity values were observed to extend to about 12 cm from the walls of the wooden tank. Resistivity measurements were therefore limited to within 14 cm from the walls.

To serve as control (baseline data), pre-impact resistivity profiles with Wenner array data were acquired for electrode spacings of 2 and 4 cm and gradient array data with a = 4 cm. In addition, axial dipole-dipole data with an expansion factor (n) varying from 1 to 5 were acquired. The station-station separation of 2 cm was used for all the three electrode array systems. Profiling was carried out along all the seven (7) traverses (TR1 –

TR7) used in this work (Fig. 3). After the conclusion of the pre-hydrocarbon impact measurements, the stoppers preventing the crude oil from leaking through the holes at the sides of the cylindrical tank were pulled out by means of the strings attached to the stoppers thus initiating the crude oil leakage into the sand formation. The hydrocarbon impacted sand left for about 24 hours to attain equilibrium. The sets of measurements carried out on the un-impacted sand i.e., pre-leakage of hydrocarbon, were repeated after the hydrocarbon leakage into the sand formation had been initiated. The same electrode arrays and spacing parameters were utilized.

As part of the data quality control, the following precautions were made: (i) the upper segment of the copper wire electrodes was rubber-insulated so as to minimize the electrode contact resistance with the resistive wooden platform, (ii) electrodes were planted firmly on the sand in order to avoid error due to soil contact effect, (iii) measurements were taken as fast as possible to avoid resistivity variations due to evaporation, (iv) instruments and cables were checked regularly to avoid malfunctioning and current leakages.

Apparent resistivity maps for the respective electrode spacings were prepared. These maps were expected to provide information on the extent of pollution with depth within the sand formation. The dipole-dipole data were interpreted using RESIX IP2DI™ iterative inversion software. Average background and target resistivity values were used as starting parameters for the inversion. RESIX IP2DI™ calculates the theoretical response using the finite element routine developed by Rijo (1977). The procedure is similar to that described by Dey and Morrison (1979) and Hohmann (1982) in which a two-dimensional finite difference or finite element algorithm is used to iteratively compute the resistivity response of a two-dimensional model, until a theoretical pseudosection is found which reasonably matches the observed one. Figure 4 is a flow chart to illustrate the RESIX IP2DI™ inversion procedure.

RESULTS AND DISCUSSION

The results of the Wenner and gradient array resistivity measurements are presented as profiles and maps, while the dipole-dipole measurement are presented as maps and pseudosections.

WENNER ARRAY PROFILES

The apparent resistivity profiles for electrode spacing a = 4 cm, for pre and post hydrocarbon impacted sand are presented in Fig. 5. The apparent resistivity values of the pre impact response generally vary from 340 to 540 ohm-m. A central relatively high

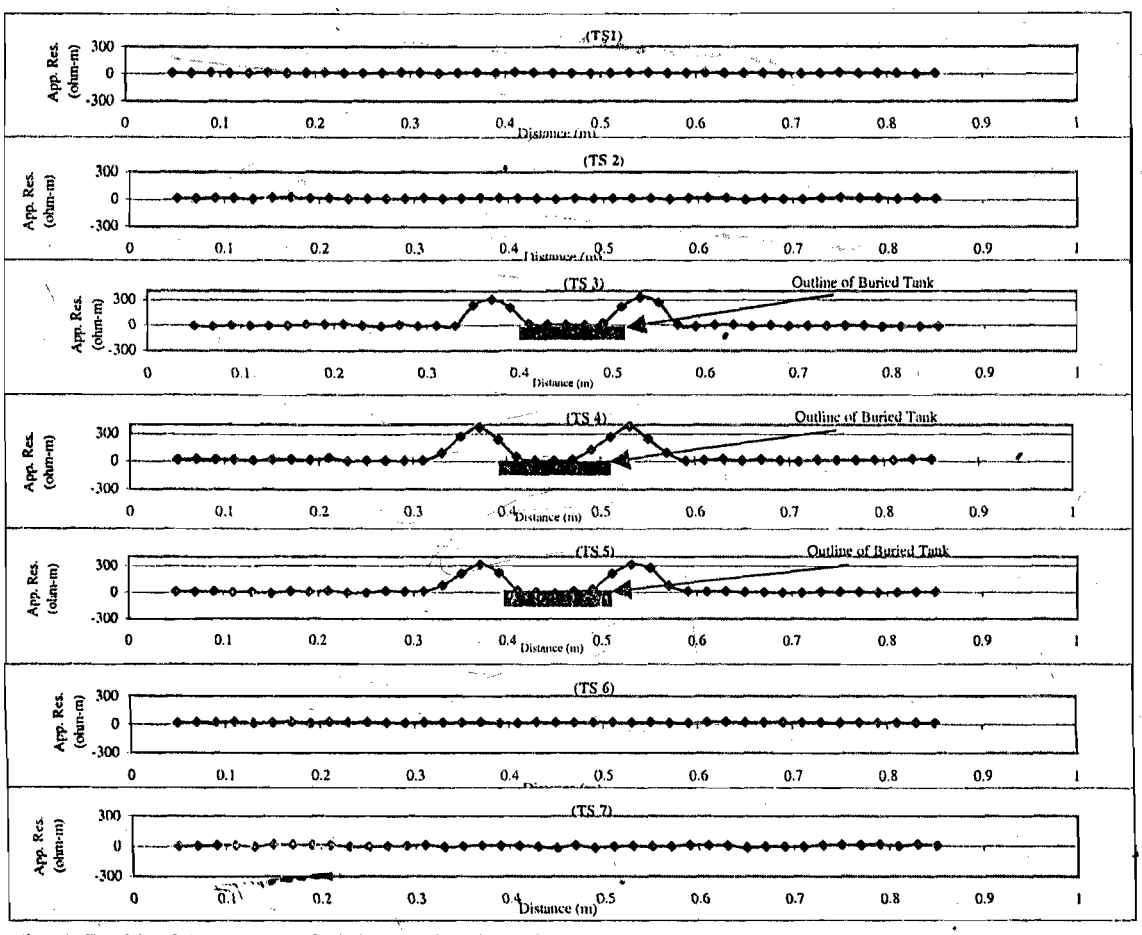

Fig. 6: Residual Wenner resistivity (a=4 cm) profiles.

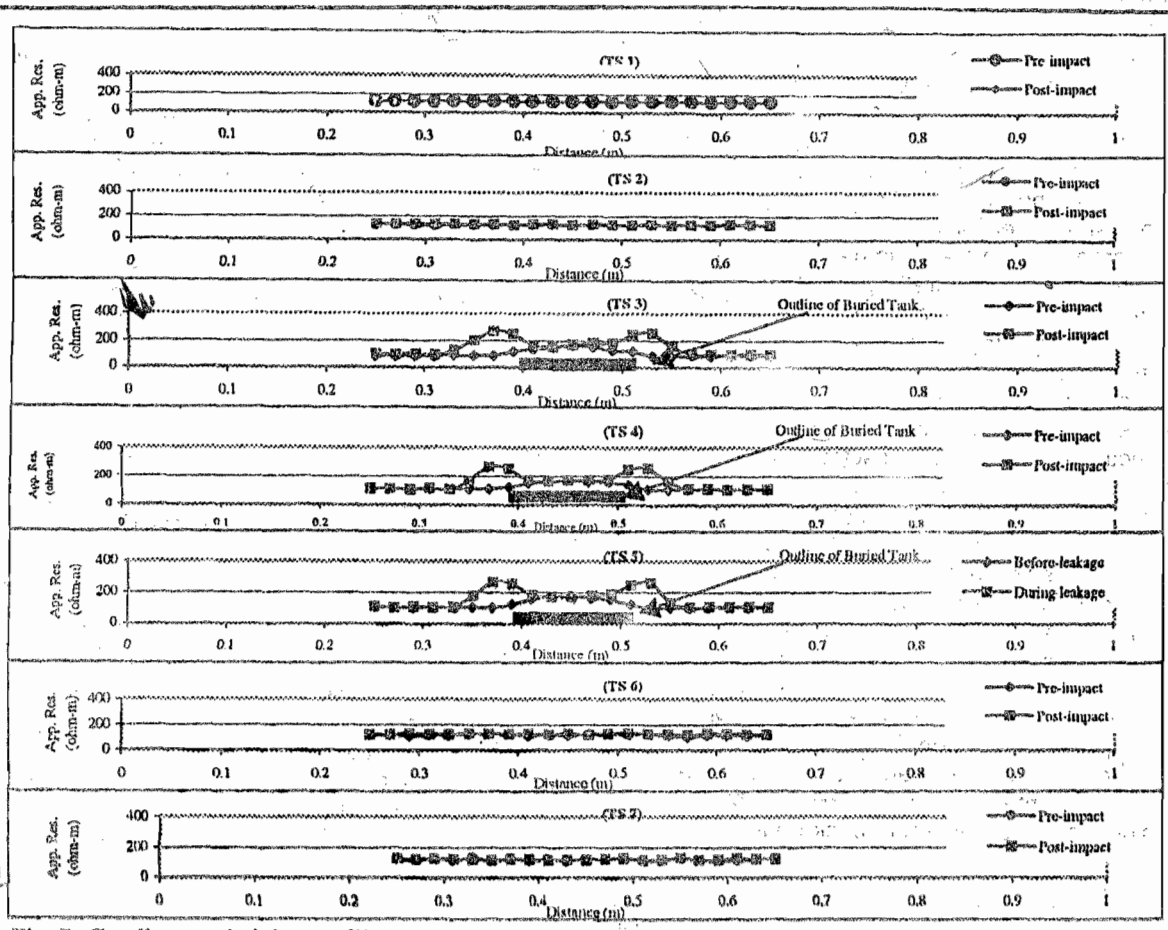

Fig. 7: Gradient resistivity profiles

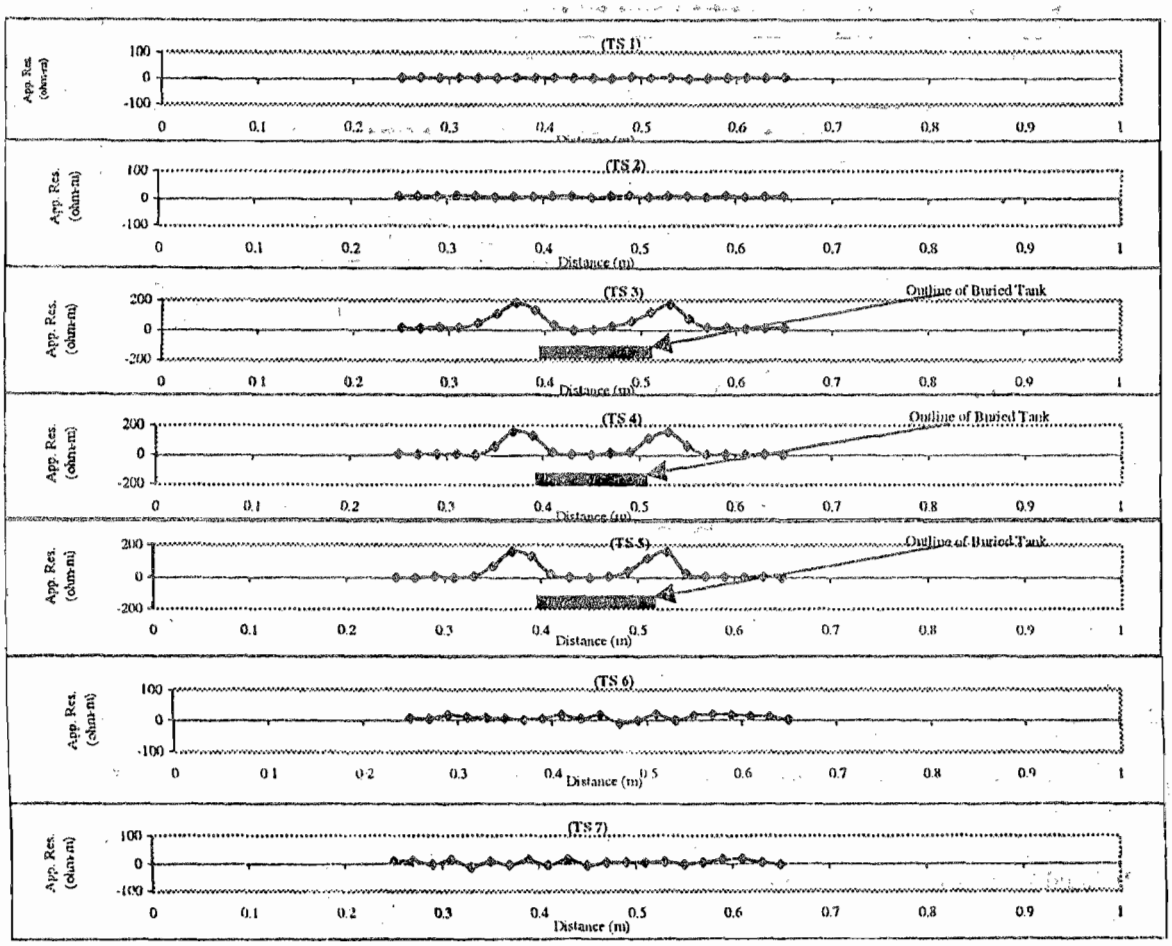

Fig. 8: Residual gradient resistivity profiles

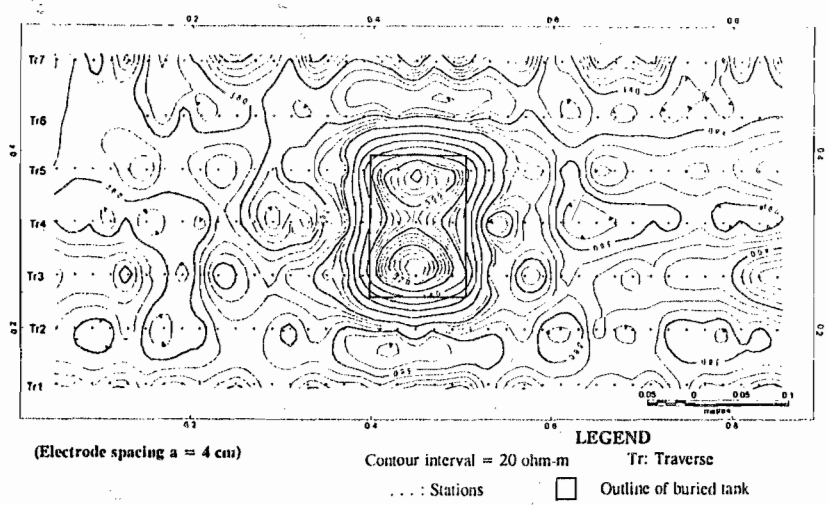

Figure 9: Wenner resistivity map of pre hydrocarbon impacted sand

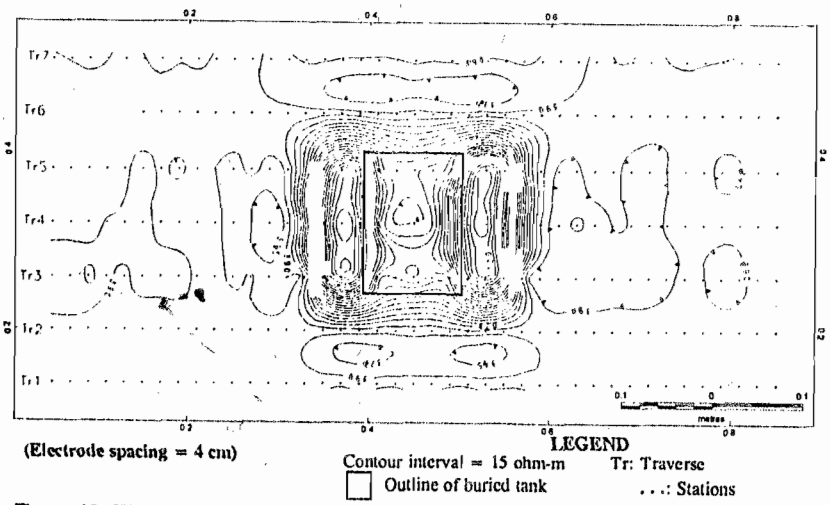

Figure 10: Wenner resistivity map of post hydrocarbon impacted sand

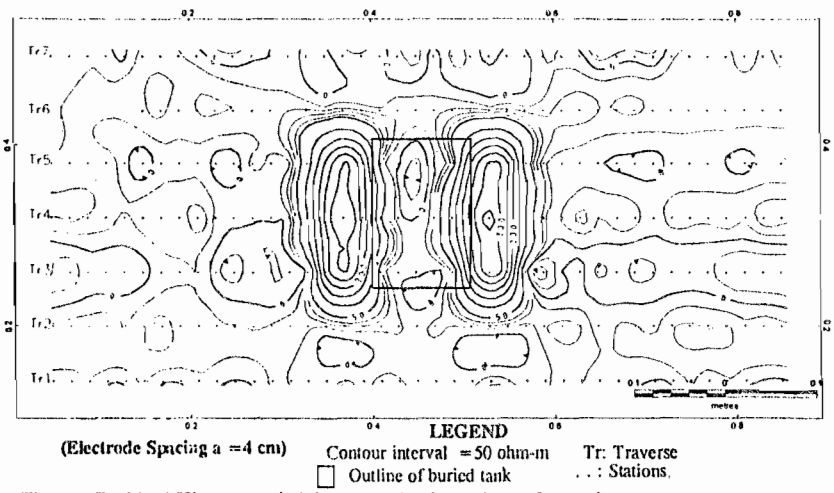

Fig. 11: Residual Wenner resistivity map of a 4 cm electrode spacing

apparent resistivity response was observed on the buried tank along traverses 3, 4 and 5 with apparent resistivity values ranging from 372 – 540 ohm-m, 372 – 497 ohm-m, and 378 – 523 ohm-m respectively. The anomalous zone, indicating the position of the buried tank has a lateral extent of about 13 cm, which compares well with the actual diameter of the tank. The apparent resistivity profiles obtained along traverses 1, 2, 6 and 7 outside the buried tank also show a fairly uniform resistivity values that averaged 350 ohm-m.

The post-impact apparent resistivity response along traverses 3, 4 and 5 varies from 374 – 724 ohm-m, 362 – 753 ohm-m and 381 – 754 ohm-m respectively. These three traverses show three regions whose resistivity values are relatively higher than that of the surrounding. A central apparent resistivity high with

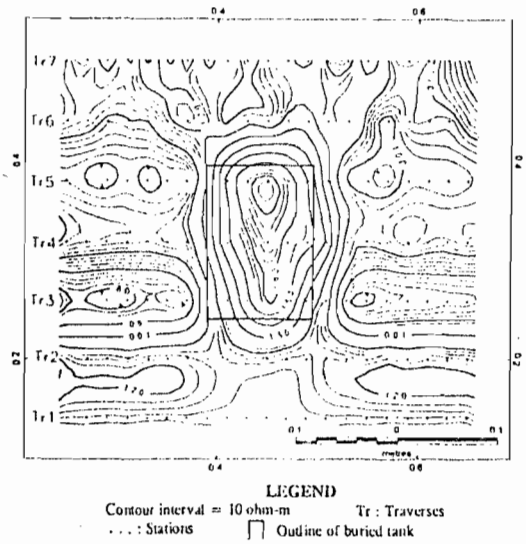

Fig. 12: Gradient resistivity map of pre hydrocarbon impacted sand

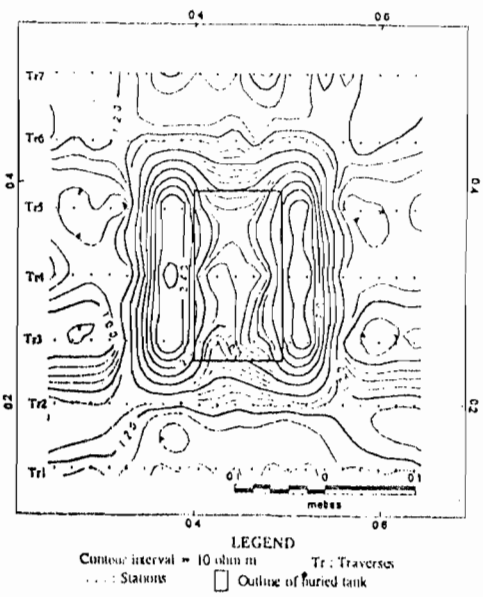

Fig. 13: Gradient resistivity map of hydrocarbon impacted sand

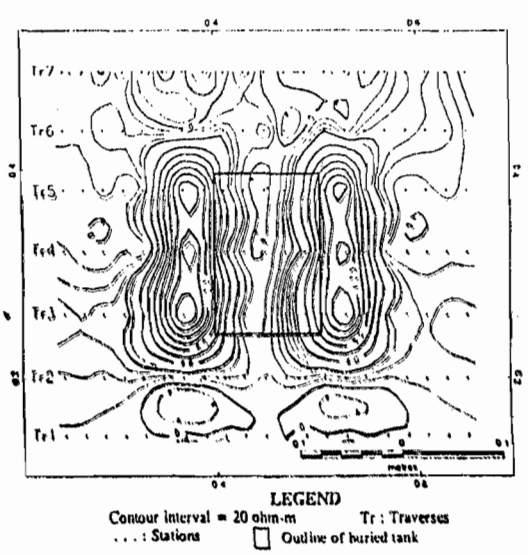

Fig. 14: Residual gradient resistivity map over sand

peak values of 520 ohm-m, 499 ohm-m and 518 ohm-m indicating the position of the buried tank is flanked on either side by two regions with higher amplitude peak resistivity values of 714 ohm-m, 753 ohm-m and 745 ohm-m respectively. The region bounded by this relatively high apparent resistivity can be seen to span about 5 cm, 8 cm and 6 cm along Traverses 3, 4 and 5 respectively. These regions show the extent of the impacted zone. The zone of hydrocarbon impact can also be clearly seen on the residual profiles (Fig. 6). The anomalously high apparent resistivity zones are indicative of the hydrocarbon-impacted sand. Traverses 1, 2, 6 and 7 outside the buried tank show fairly uniform resistivity values averaging 390 ohm-m.

GRADIENT ARRAY PROFILES

The gradient array apparent resistivity profiles are presented in Fig. 7. The resistivity response curves bear close resemblance to that of Wenner array except for the relatively lower apparent resistivity values. The apparent resistivity response of the pre impact sand along traverses 3, 4 and 5 generally varies from 79 – 163 ohm-m, 104 – 169 ohm-m, and 98 – 173 ohm-m respectively. A zone of relatively high apparent resistivity values reaching peak amplitudes of 163 ohm-m, 169 ohm-m and 173 ohm-m respectively can be observed at the central part. This anomalous zone spans about 13 cm and delineate the position of the buried tank. The post hydrocarbon impacted sand gradient array resistivity profiles are also displayed in Fig. 7.

The post impact apparent resistivity response along traverses 3, 4 and 5 varies from 93 – 266 ohm-m, 104 – 266 ohm-m and 100 – 260 ohm-m respectively. Traverses 3, 4 and 5 are characterized by three regions whose resistivity values are relatively higher than that of the surrounding. A central apparent resistivity high with peak values of 169 ohm-m, 170 ohm-m and 172 ohm-m is flanked by two regions with peak values of 266 ohm-m, 266 ohm-m and 260 ohm-m respectively along traverses 3, 4 and 5. The anomalous apparent resistivity zones span approximately 5 cm, 6 cm and 5 cm along traverses 3, 4 and 5 respectively. These regions show the extent of the impacted sand. The hydrocarbon-impacted zone is well displayed on the residual profiles (Fig. 8). The anomalously high apparent resistivity zone is diagnostic of hydrocarbon-impacted sand. Traverses 1, 2, 6 and 7 outside the buried tank show fairly uniform resistivity values averaging 100 ohm-m.

WENNER ARRAY MAPS

The Wenner apparent resistivity contour map for electrode spacing a = 4 cm, for the pre-impact sand is presented in Fig. 9. The buried tank is characterized by a central high resistivity closure with a threshold of 480 ohm-m. Fig. 10 shows the post impact Wenner resistivity contour map. The map is characterized by two high resistivity closures enclosing a central relatively low (less 540 ohm-m) resistivity zone located over the buried tank. The two flanking high resistivity zones are diagnostic of the hydrocarbon-impacted zones.

The resistivity residual map (Fig. 11) also identifies the two hydrocarbon impacted zones flanking the central buried tank as two anomalously high resistivity closures relative to the low resistivity closure observed on the buried tank.

GRADIENT ARRAY MAPS

The gradient array resistivity contour maps are presented in Figures 12 – 14. The resistivity map for the pre-impact sand is presented in Fig.12. The map shows apparent resistivity contours varying from 80 ohm-m to 170 ohm-m. The map is characterized by relatively high apparent resistivity contour closures at the center of the map with a fairly uniform low apparent resistivity (less than 120 ohm-m) background. Figure 13 shows the apparent resistivity contour map of the hydrocarbon-impacted sand. The map is characterized by two high resistivity contour closures enclosing a central resistivity low overlying the buried tank. The relatively high apparent resistivity closures show the regions of hydrocarbon impact. The residual apparent resistivity contour map (Fig.14) shows anomalously high resistivity contour closures over the hydrocarbon impacted.

DIPOLE – DIPOLE ARRAY MAPS

Figures 15 - 19 show the dipole – dipole apparent resistivity maps for the expansion factors n = 1 – 5 over the pre hydrocarbon impacted sand. The ranges of apparent resistivity values are approximately 380 – 460 ohm-m, 360 – 680 ohm-m, 380 – 620 ohm-m, 380 – 620 ohm-m and 380 – 850 ohm-m, for n = 1 – 5 respectively. The buried tank is characterized by central high resistivity closures. The extent of the closures are however slightly wider than that of the tank.

Figures 20 - 24 show the dipole – dipole apparent resistivity maps for n 1 – 5 over the post impacted sand. The ranges of apparent resistivity values are 400 – 900 ohm-m for n = 1 to 4 and 400 – 1200 ohm-m, for n = 5. Three distinct regions can be recognized on each of the maps. The most prominent are the two high resistivity closures (> 400 ohm-m) enclosing a central relatively low resistivity zone overlying the buried tank. The two high resistivity closures are indicative of the hydrocarbon-impacted zones.

DIPOLE – DIPOLE PSEUDOSECTIONS

The dipole-dipole pseudosections and the inverted interpretation models are presented in Figs 25 – 30. Figures 25 – 27 show the pseudosections and the geoelectric models of the pre-impact resistivity response along Traverses 3 – 5 respectively. The pseudosections generally show a similar pattern and apparent resistivity values from 350 ohm-m in most places to 850 ohm-m with the anomalously high resistivity zone located on the buried tank.

The geoelectric sections of the pre – impact sand (Figs 25 – 27) show a circular outline representing the cross section of the buried tank. The approximate diameter of the tank from the model is 14cm. The outline

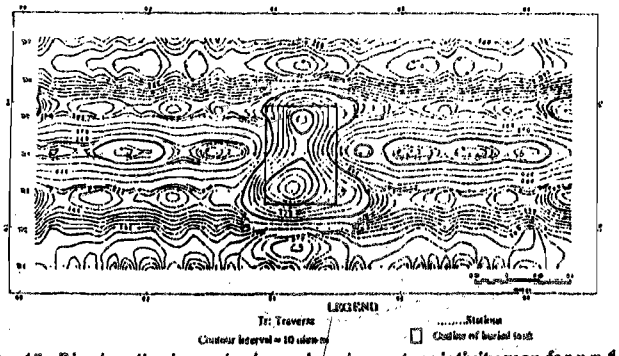

Fig. 15: Dipole - dipole pre hydrocarbon impact resistivity map for n = 1

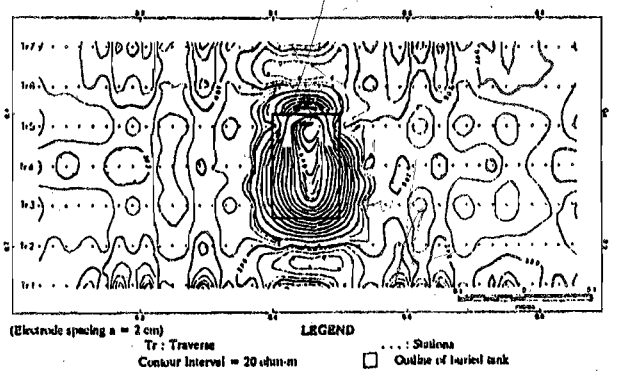

Fig. 16: Dipole-dipole pre hydrocarbon impact resistivity map for n = 2

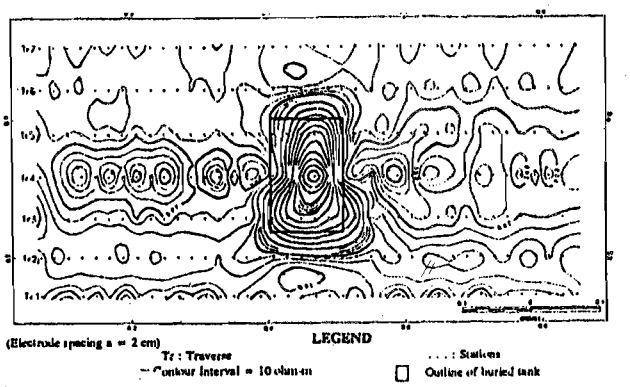

Fig. 17: Dipole-dipole pre hydrocarbon impact resistivity map for n = 3

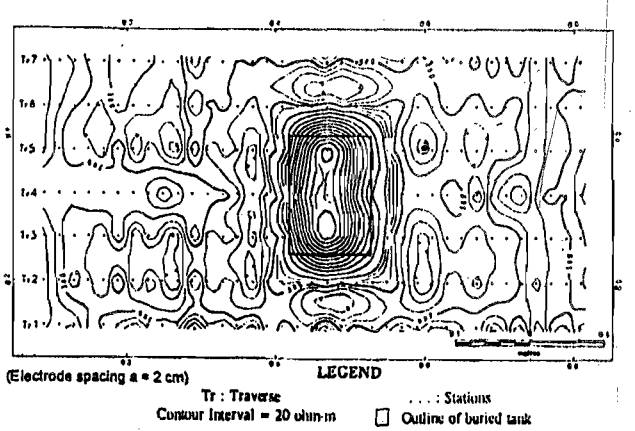

Fig. 18: Dipole-dipole pre hydrocarbon impact resistivity map for n = 4

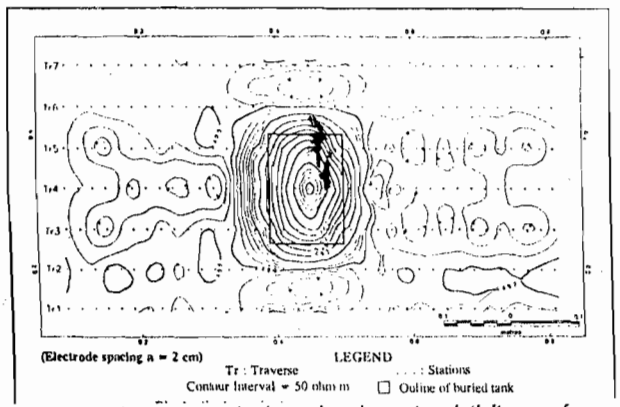

Fig. 19: Dipole-dipole pre hydrocarbon impact resistivity map for n = 5

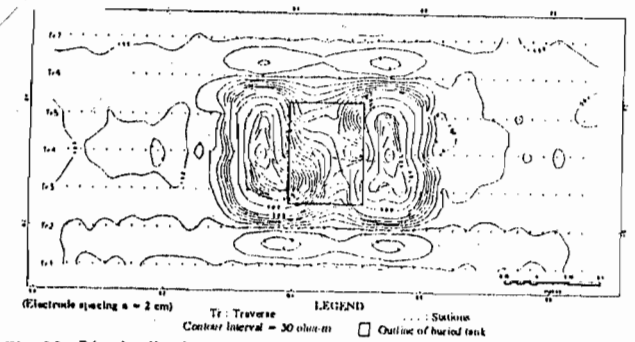

Fig. 20: Dipole-dipole post hydrocarbon impact resistivity map for n = 1

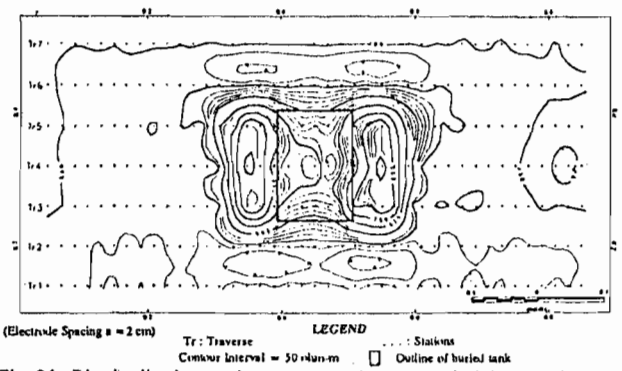

Fig. 21: Dipole-dipole post hydrocarbon impact resistivity map for n = 2

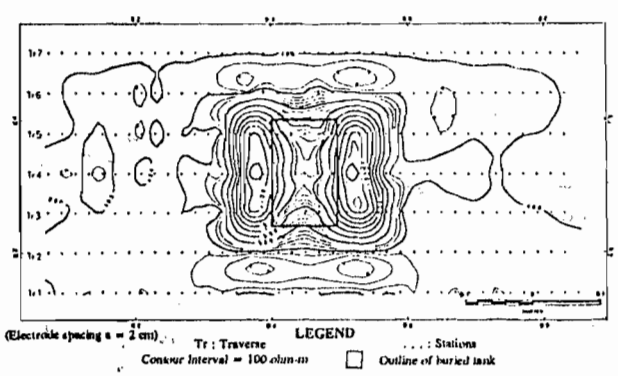

Fig. 22: Dipole-dipole post hydrocarbon impact resistivity map for n = 3

of the tank can also be observed to be ellipsoidal rather than circular. This effect is due to the vertical exaggeration, which is approximately 5 for all the models. Since the actual diameter of the tank is 13.2 cm, there is a slight over estimation of the diameter as determined from the geoelectric section. The depth to

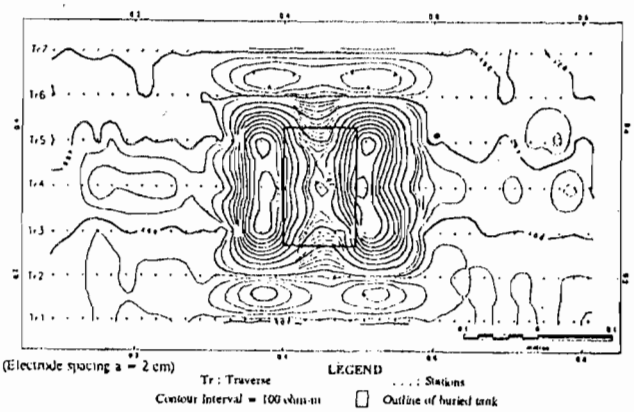

Fig. 23: Dipole-dipole post hydrocarbon impact resistivity map for n = 4

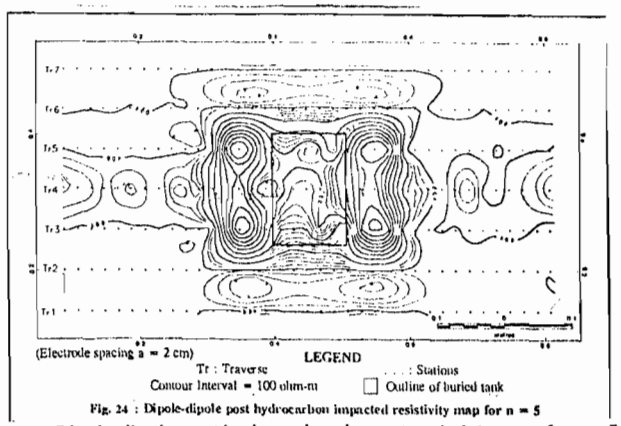

Fig. 24: Dipole-dipole post hydrocarbon impact resistivity map for n = 5

the top surface of the buried tank is approximately 2.42 cm, 2.36 cm and 2.38 cm from the top of the sand on traverse 3 to traverse 5 respectively. However, the actual depth is 2.5 cm. This shows a slight under estimation of the depth to the top surface of the buried tank. The largest error of 12.22% was recorded along traverse 5.

The dipole-dipole pseudosections obtained over hydrocarbon-impacted sand are shown in Figures 28 – 30. The apparent resistivity values vary from 360 ohm-m - 1200 ohm-m. The hydrocarbon-impacted zones are delineated as high resistivity zones. The interpreted models identified two degrees of impact. The heavily impacted zone with apparent resistivity values > 1000 ohm-m is located at the center. The heavily impacted zone is bordered by a slightly impacted zone with resistivity values < 1000 ohm-m. Figure 31 shows the extent of the pollution plume as derived from the geophysical interpretation.

ESTIMATION OF VOLUME LEAKED HYDROCARBON.

The volume of leaked hydrocarbon can be determined from depth values obtained from modelled dipole-dipole pseudosections and average laboratory determined porosity of sand. If it is assumed that the geometry of the hydrocarbon impacted zone is ellipsoidal, and the interstitial spaces of the impacted zone are completely filled with hydrocarbon,

The volume (V) of the impacted area is given by Equation 1.

$$V = \frac{4}{3}\pi abc \qquad (1)$$

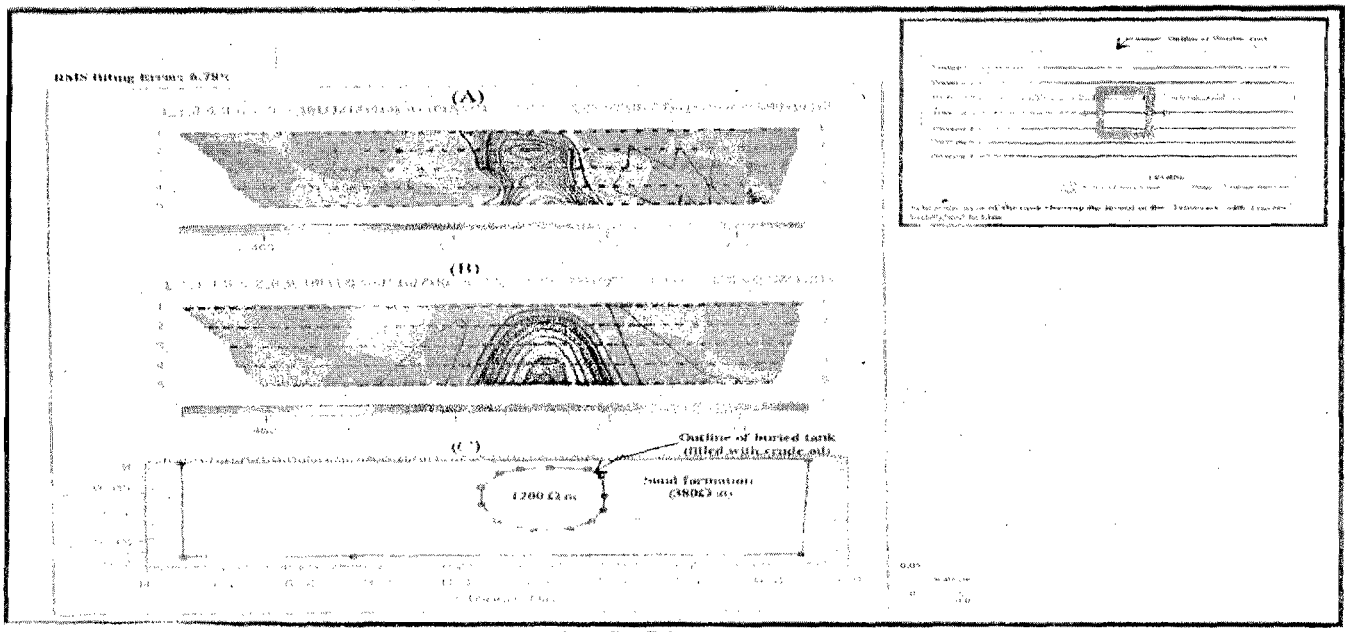

Fig. 25: (A) Measured dipole-dipole pseudosection, (B) Calculated dipole-dipole pseudosection and (C) Inverted model section of pre-impact sand along Traverse 3.

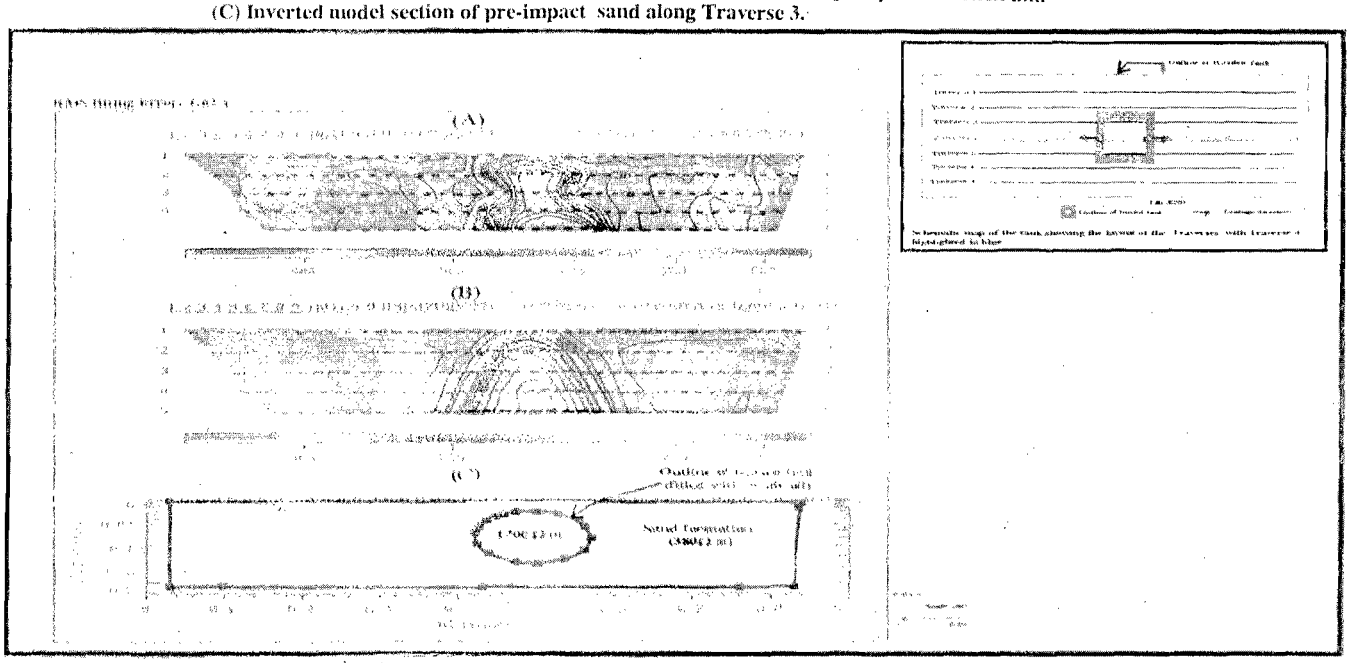

Fig. 26: (A) Measured dipole-dipole pseudosection, (B) Calculated dipole-dipole pseudosection and (C) Inverted model section of pre-impact sand along Traverse 4.

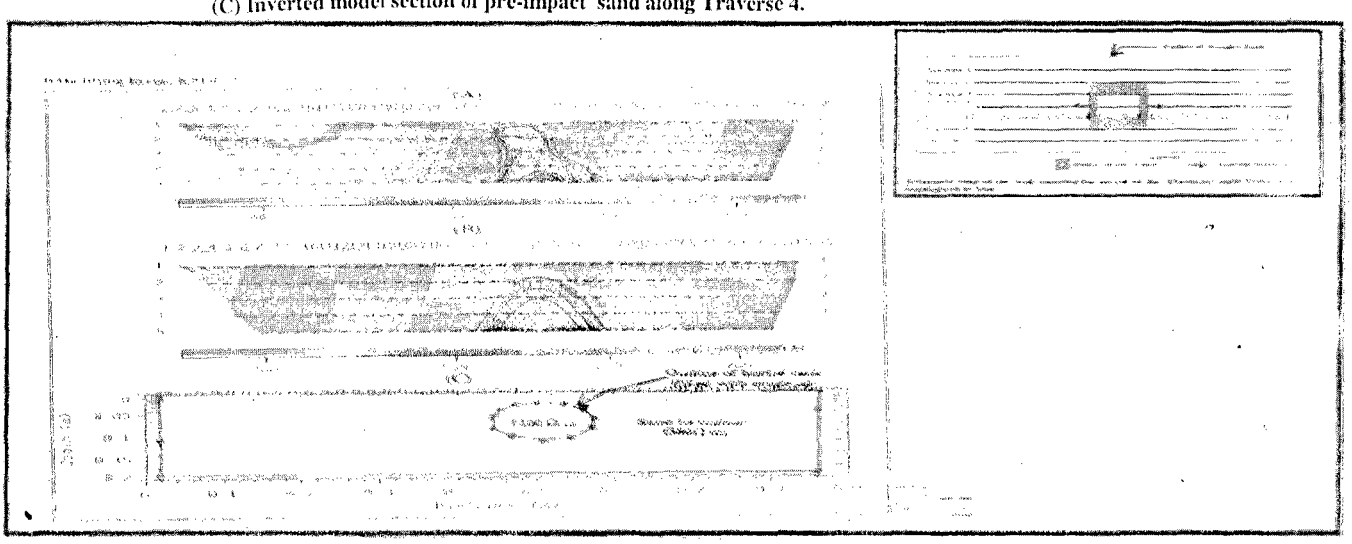

Fig. 27: (A) Measured dipole-dipole pseudosection, (B) Calculated dipole-dipole pseudosection and (C) Inverted model section of pre-impact sand along Traverse 5.

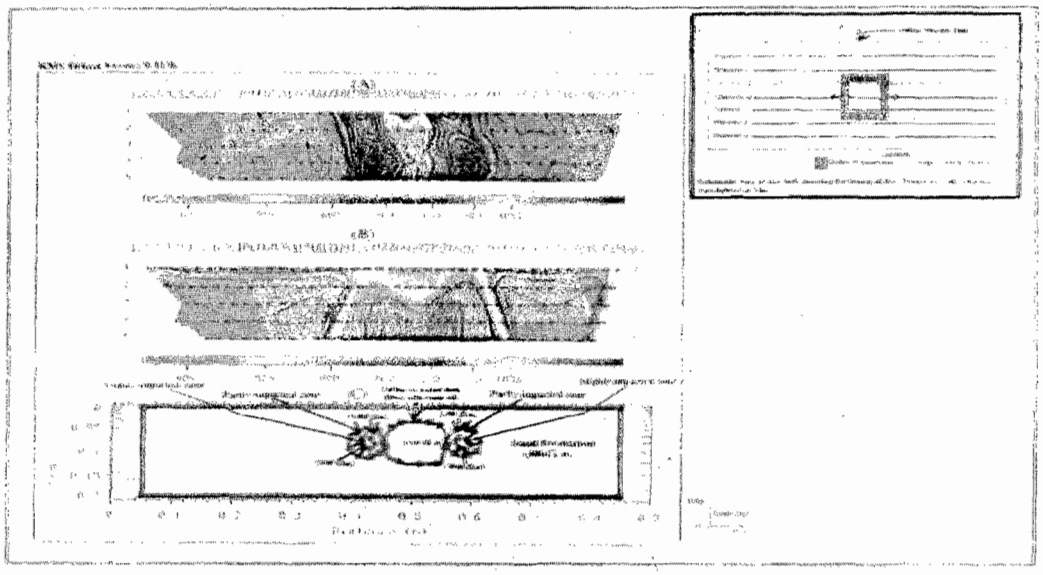

Fig. 28: (A) Measured dipole-dipole pseudosection, (B) Calculated dipole-dipole pseudosection and (C) Inverted model section of post-impact sand along Traverse 3.

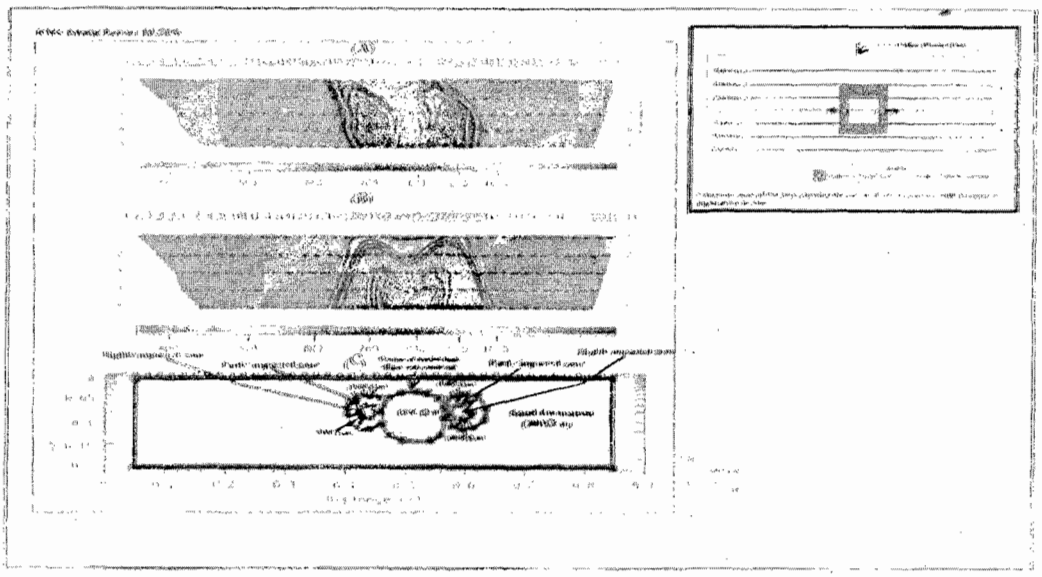

Fig. 29: (A) Measured dipole-dipole pseudosection, (B) Calculated dipole-dipole pseudosection and (C) Inverted model section of post-impact sand along Traverse 4.

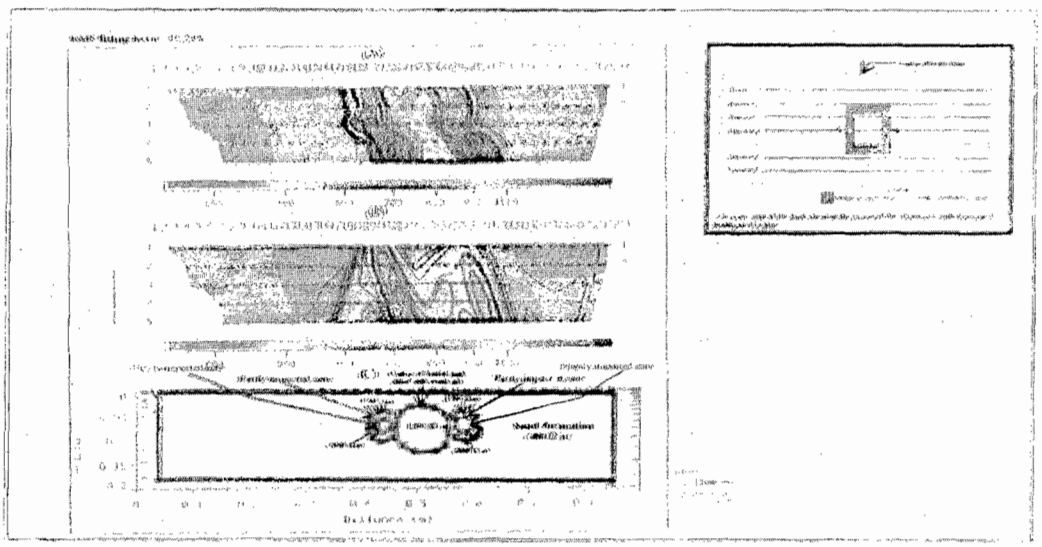

Fig. 30: (A) Measured dipole-dipole pseudosection, (B) Calculated dipole-dipole pseudosection and (C) Inverted model section of post-impact sand along Traverse 5.

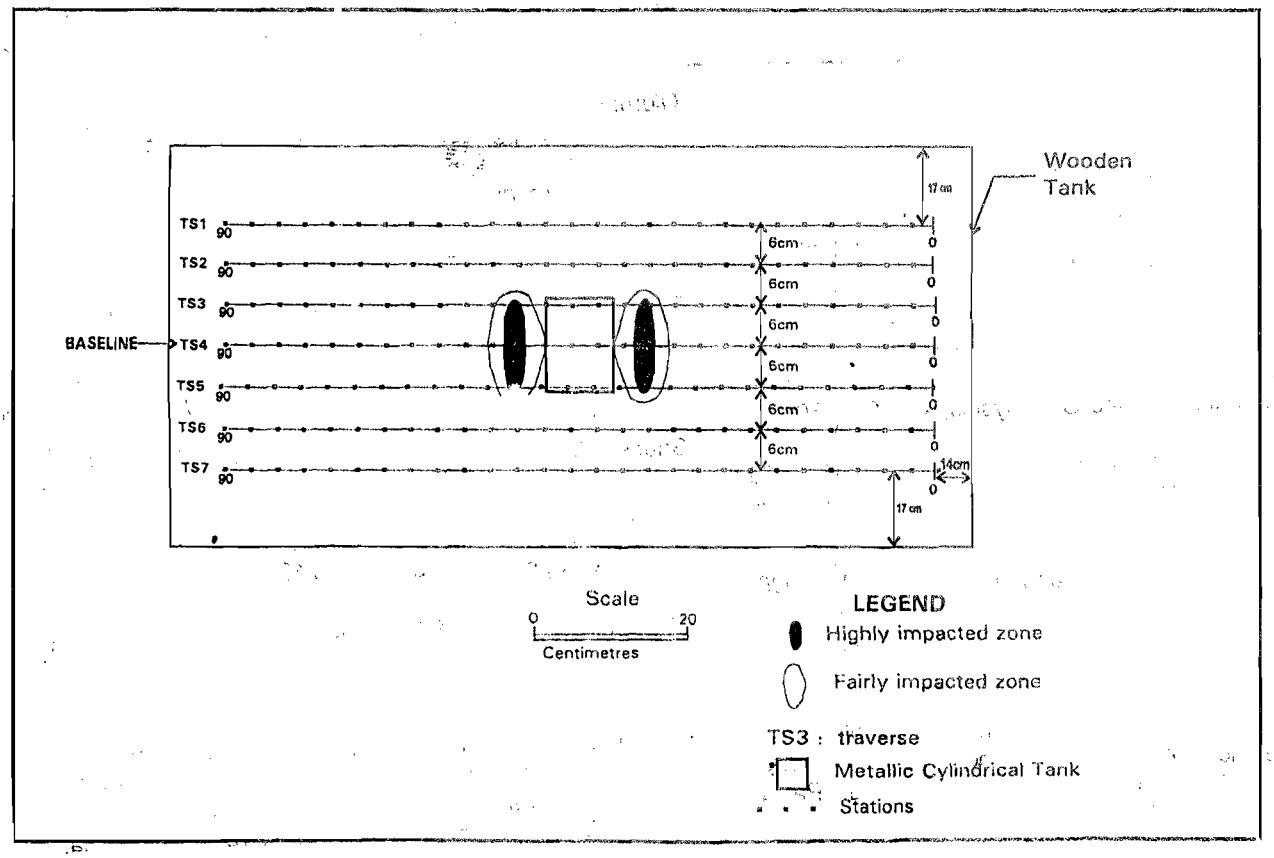

Figure 31: Map of the tank showing the layout of the traverses and the impacted zone derived from combined interpretation and the modelling.

Where the lengths of the semi axes are represented by a, b and c. Where from Fig.31, a = 8 cm, b = 3.63 cm and c = 4 cm

Therefore, the volume of the leaked hydrocarbon V_L at the time of post impact measurement is given by:

$$V_L = \phi V \quad (2)$$

Where the porosity, ϕ = 33%

The volume of leaked hydrocarbon estimated from the forgoing is 161 cm^3. The leakage however, occurred on two sides of the tank. Since the geometry of the two sides are similar and porosity same, it implies that the total volume of leaked hydrocarbon is 322 cm^3, i.e., 13.6% of the 2368 cm^3 present in the buried tank had leaked into the surroundings at the time of measurement. This implied that the hydrocarbon leaked at approximately 7 cm^3/hr from the side of tank.

CONCLUSIONS

In this paper a non-invasive geophysical technique based on electrical tomography has been applied to determine the lateral and depth extent of a simulated leaking buried petroleum tank. The results indicate that the hydrocarbon-impacted sand is identified by high resistivity anomaly. The anomaly is identified by any of the three arrays used for measurement. Therefore, the electrical resistivity method utilizing either the Wenner, Dipole-Dipole or the Gradient array can be used to investigate subsurface pollution, estimate volume of impacted hydrocarbon as well as the source of the impact particularly in typically sandy areas.

The method can reduce or eliminate the risks of undetected targets and to expedite site characterization by providing 2D/3D images of changes in apparent resistivity contrasts in the subsurface. Also, site screening is optimized in advance of follow-up drilling and sampling which, therefore, deliver a more effective and representative analysis of subsurface contamination. For the effective use of electrical resistivity method and other relevant geophysical methods in environmental impact assessments (EIA), baseline study is a necessary pre-requisite.

ACKNOWLEDGEMENTS

The authors acknowledge the Shell Professor of Geophysics Department of Geology (Prof. B.D. Ako) Obafemi Awolowo University Ile-Ife, for providing the necessary computer hard- and soft-wares used in this work.

REFERENCES

Akinluyi, F.O., 2000. Laboratory modelling of geoelectric responses of hydrocarbon impacted sand formation. Unpubl. M.Sc Thesis, Obafemi Awolowo University Ile-Ife. pp.154.

Atekwana, E.A., Sauck, W.A., and Werkama, D.D. 2000. Investigations of geoelectrical signatures at hydrocarbon contaminated site. Journal of Applied Geophysics, 44: 167- 180.

Dey, A. and Morrison, H.F., 1979. Resistivity modelling of arbitrarily shaped bodies. Geophysics, Vol. 27: 1030 – 1036.

Gibson, P. J., Lyle, P. and George, D.M. 1996. Environmental applications of magnetometry profiling. Environmental Geology and Water Sciences, 27: 178-183.

Hohmann, G.W., 1982. Numerical modelling for electrical geophysical methods. Proc. Int. Symp. Appl. Geophyiscs, Trop., Reg., Univ. do Parra. Belem, Brazil, p. 308-304

Mazac, O. Kelly, W. E. and Landa, I. (1987). Surface geoelectrics for groundwater pollution and protection studies. Journal of Hydrology, 93: 277-294.

Olorunfemi M.O., 2001. Geophysics as a tool in Environmental Impact Assessment. Paper presented at workshop on Environmental impact Assessment, NACETEM, O.A.U. Ile-Ife. May, 2001.

Olorunfemi M.O., Olayinka, A.I. and Akinluyi, F.O. 2000. Laboratory modelling and inversion of the 2- Dimensional geoelectric response of a hydrocarbon impacted sand formation. Global Journal of Pure and Applied Sciences, 7, (4): 695 – 705.

Rijo, L. (1977). Modelling of electric and electromagnetic data. Ph.D Thesis, University of Utah, University Microfilms International, Ann Arbor, Michigan, 1997.

Sauck, W.A. Atekwana, E.A. and Nash, M.S. 1998. High conductivityies associated with an LNAPL plume imaged by integrated geophysical techniques. Journal of Environmental Geophysics, 2 (3): 203 – 212.

Steeples, D. W. 1991. Uses and techniques of environmental geophysics. The Leading Edge, 30: 30-31.

Svoma, J., 1978. Location and area measurement of Nok groundwater oil contamination by surface methods: Proc. Int. Symp. IAH on groundwater pollution by oil hydrocarbons, Praha, P. 309-317.

Vickery, A. C. and Hobbs, A. B., 1998. Contribution of surface geophysics to environmental site investigation of former oil distribution terminals. JEEG, 3 (3): 101-109.